Supporting Information

Assembling Organic-Inorganic Building Blocks for High-Capacity Electrode Design

Xiaolin Zhao[a,b,c], Zhongli Hu[d], Yining Li[a,b,c], Youwei Wang[a,b,c], Erhong Song[a,b,c], Li Zhang[d], Jianjun Liu[a,b,c]**

[a]State Key Laboratory of High Performance Ceramics and Superfine Microstructure, Shanghai Institute of Ceramics, Chinese Academy of Sciences, 1295 Dingxi Road, Shanghai 200050, China

[b]Center of Materials Science and Optoelectronics Engineering, University of Chinese Academy of Sciences, Beijing 100049, China

[c]School of Chemistry and Materials Science, Hangzhou Institute for Advanced Study, University of Chinese Academy of Sciences, 1 Sub-lane Xiangshan, Hangzhou 310024, China

[d]State Key Laboratory of Physical Chemistry of Solid Surfaces, College of Chemistry and Chemical Engineering, Xiamen University, Xiamen 361005, Fujian, China.

Corresponding Author

*** E-mail Address:** zhangli81@xmu.edu.cn; jliu@mail.sic.ac.cn

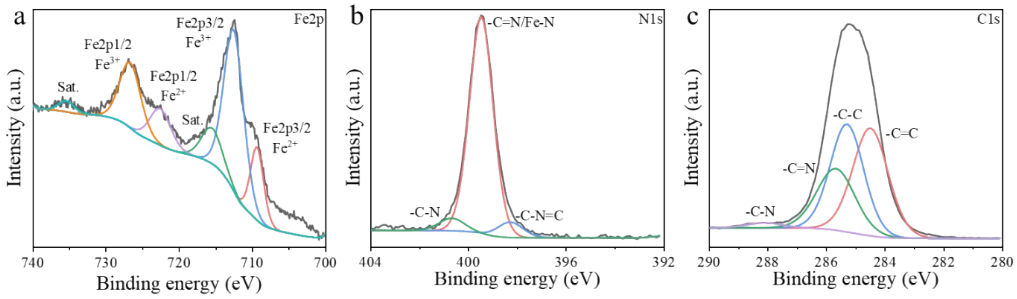

Figure S1. (a) Fe2p, (b) N1s and (c) N1s XPS spectra of FeF_3(4,4′-bpy).

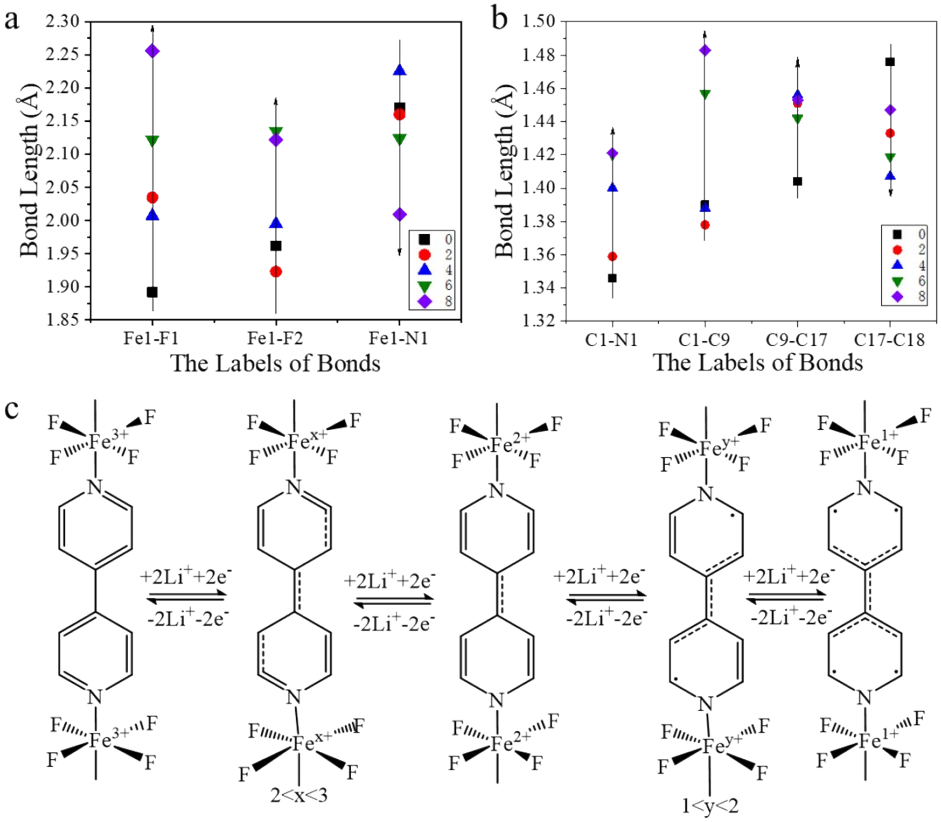

Figure S2. (a) The bond lengths of different Fe-F bonds in crystal structure of $Li_x[FeF_3(4,4'\text{-bpy})]$ (x=0, 2, 4, 6, 8). (b) The bond lengths of different C=N and C=C double bonds in crystal structure of $Li_x[FeF_3(4,4'\text{-bpy})]$ (x=0, 2, 4, 6, 8). (c) The double bond reformation of $FeF_3(4,4'\text{-bpy})$.

Table S1. The Gibbs free energy of the decomposition reaction for the Li_4FeF_3(4,4′-bpy) and Li_8FeF_3(4,4′-bpy).

	Reaction	ΔG/eV
1	$Li_4[FeF_3(4,4'\text{-bpy})] \rightarrow Li_4(4,4'\text{-bpy}) + FeF_3$	10.44
2	$Li_8[FeF_3(4,4'\text{-bpy})] \rightarrow Li_8(4,4'\text{-bpy}) + FeF_3$	11.71
3	$Li_4[FeF_3(4,4'\text{-bpy})] \rightarrow Li[Fe(4,4'\text{-bpy})] + 3LiF$	0.57
4	$Li_8[FeF_3(4,4'\text{-bpy})] \rightarrow Li_5[Fe(4,4'\text{-bpy})] + 3LiF$	2.42

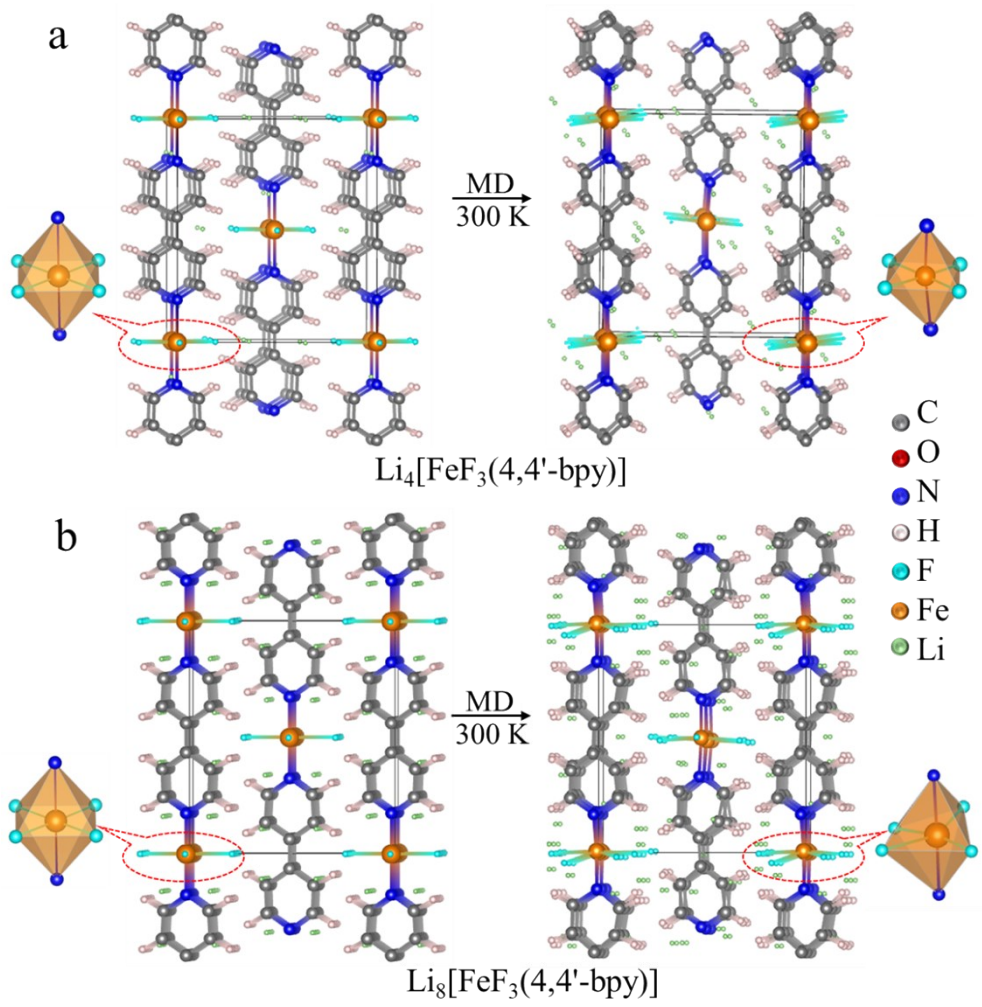

Figure S3. DFT-based molecular dynamic simulation for lithiated structures a. $Li_4[FeF_3(4,4'\text{-bpy})]$ and b. $Li_8[FeF_3(4,4'\text{-bpy})]$.

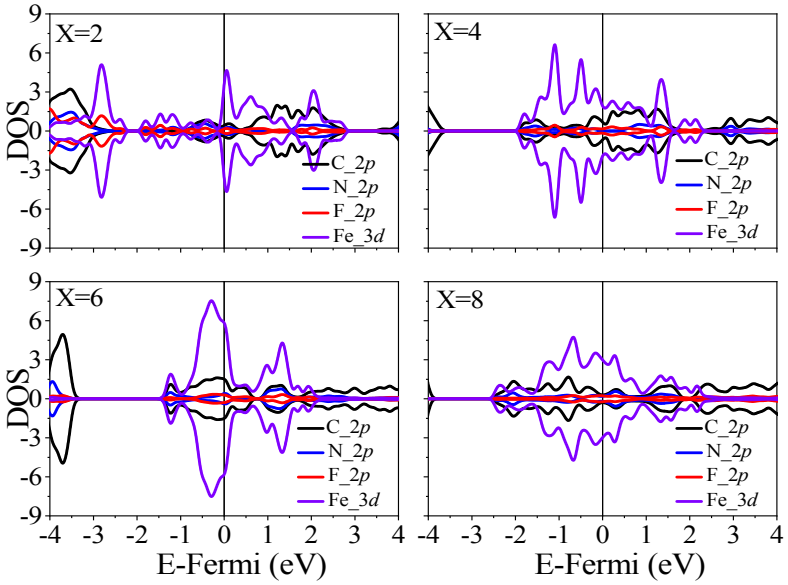

Figure S4. The projected density of states (pDOS) of $Li_x[FeF_3(4,4'\text{-bpy})]$ (x=2, 4, 6, 8).

Table S2. The magnetic moment of Fe in $Li_x[FeF_3(4,4'\text{-bpy})]$ (x=0, 2, 4, 6, 8)

$Li_x[FeF_3(4,4'\text{-bpy})]$	0	2	4	6	8
Magnetic moment	4.8	4.2	0	1.7	3.2
Spin state	High spin	High spin	Low spin	High spin	High spin
Electron number of d	$d^{5.2}$	$d^{5.8}$	d^{6}	$d^{6.3}$	$d^{6.8}$
Valence of Fe	+2.8	+2.2	+2	+1.7	+1.2

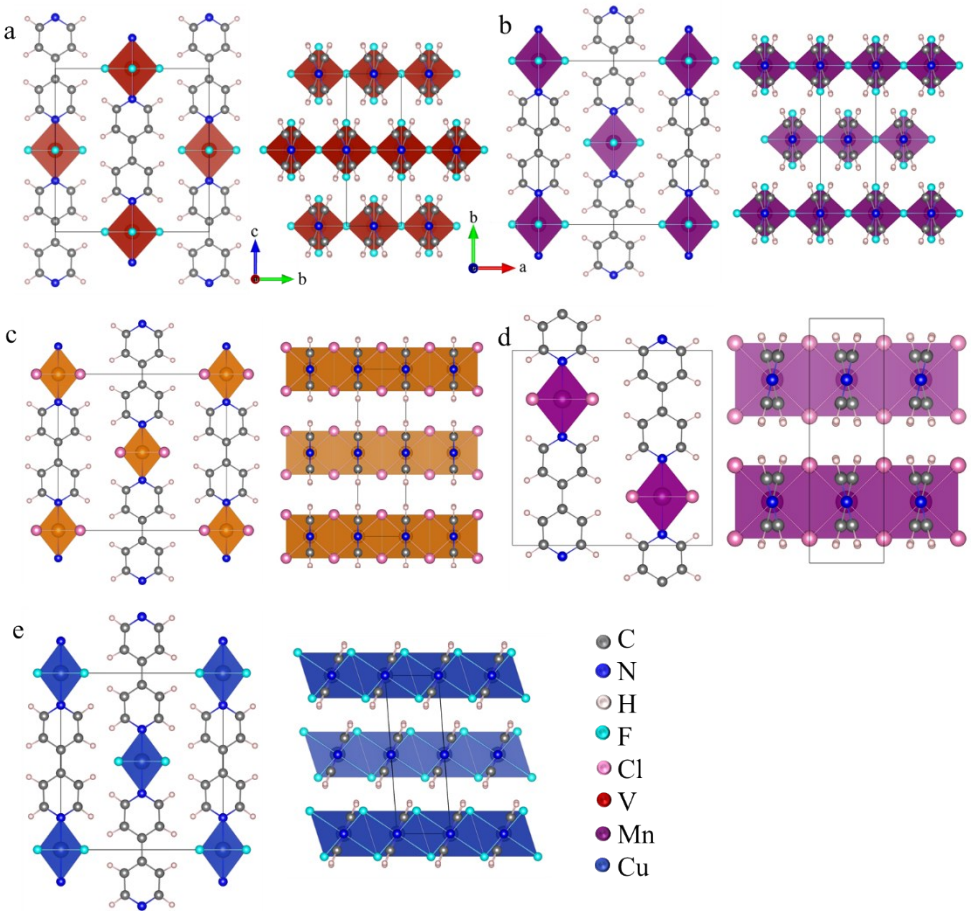

Figure S5. The crystal structure of (a) VF_3(4,4′-bpy) (b) MnF_3(4,4′-bpy) (c) $FeCl_2$(4,4′-bpy) (d) $MnCl_2$(4,4′-bpy) (e) CuF_2(4,4′-bpy) along (100) direction and (001) direction. VF_3(4,4′-bpy)

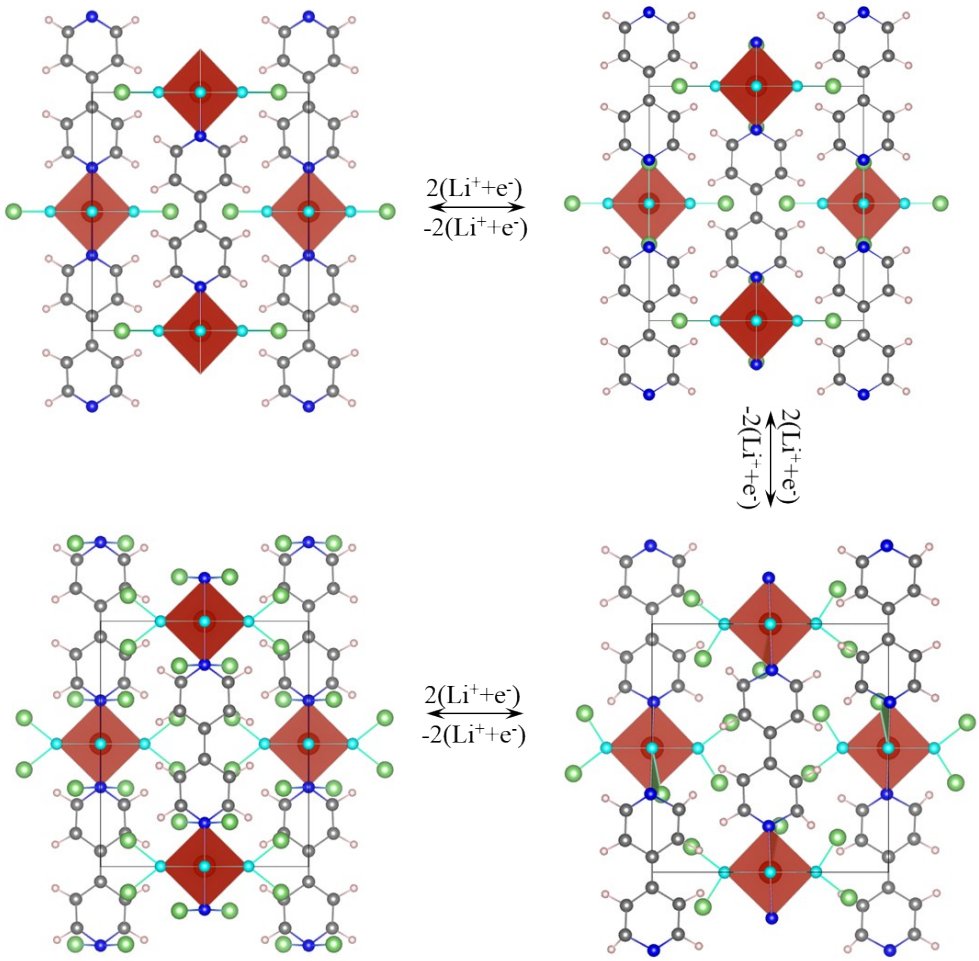

Figure S6. The Li-ions storage sites and the structural evolution in VF_3(4,4′-bpy)

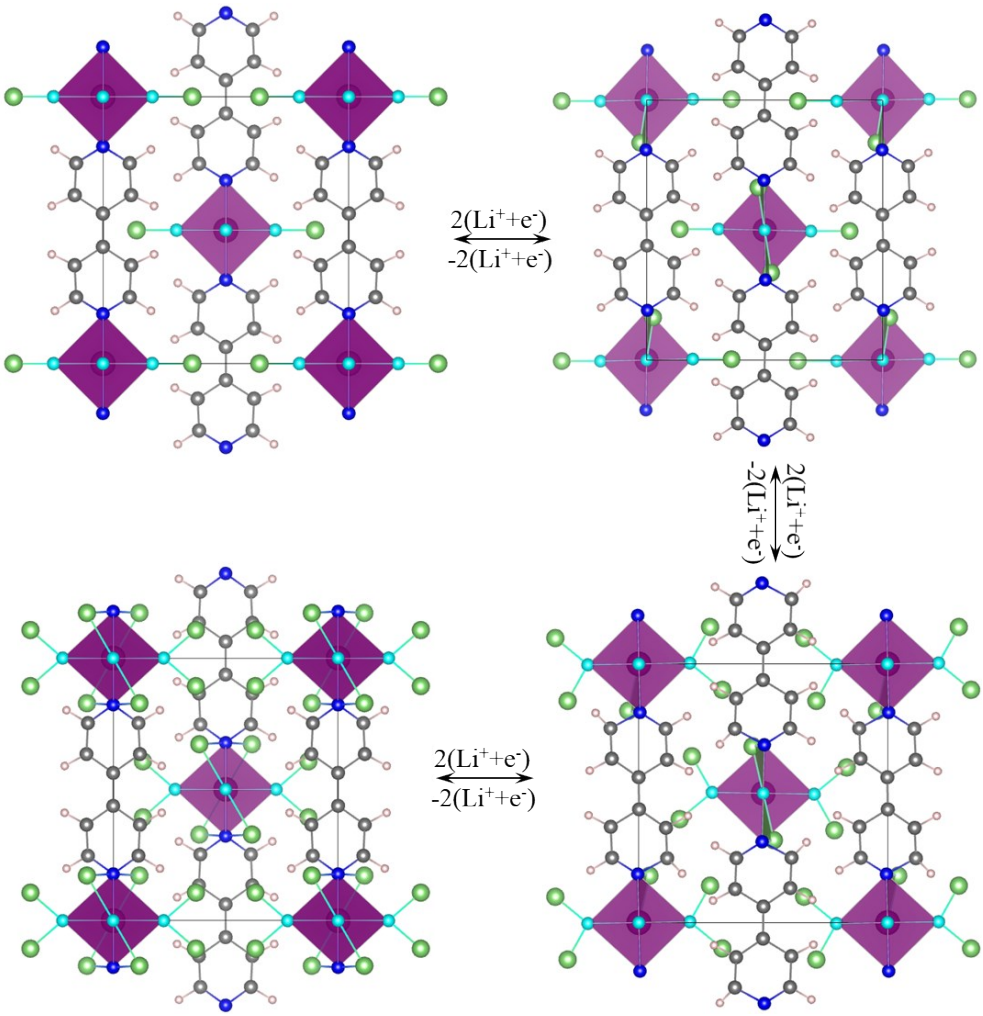

Figure S7. The Li-ions storage sites and the structural evolution in MnF_3(4,4′-bpy)

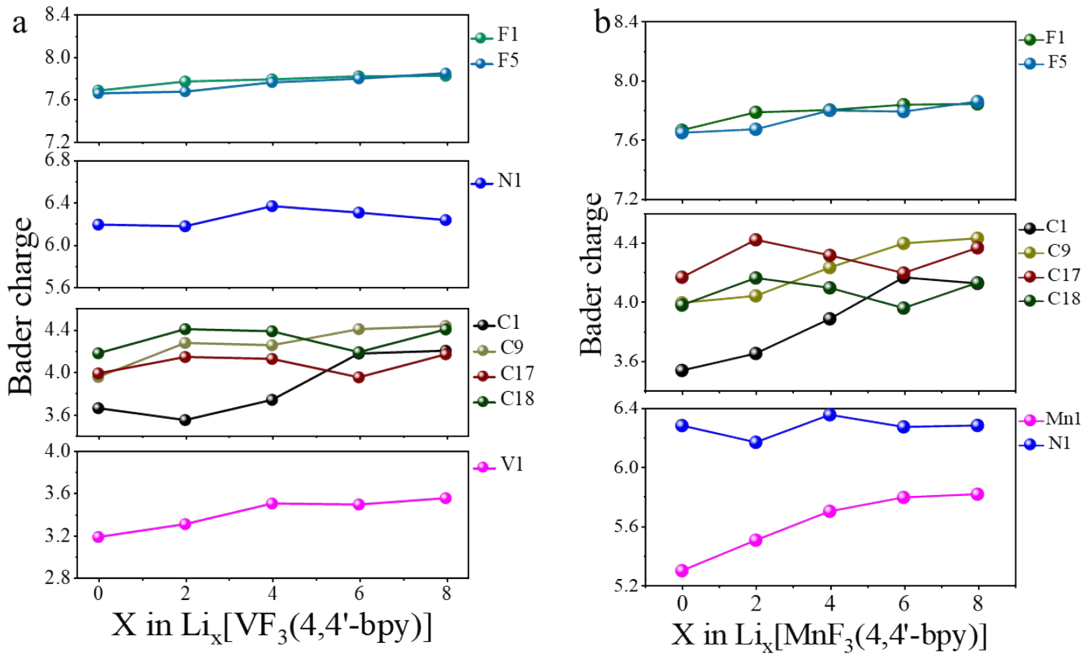

Figure S8. The change in Bader charge of (a) VF_3(4,4′-bpy) and (b)MnF_3(4,4′-bpy) during the discharge.

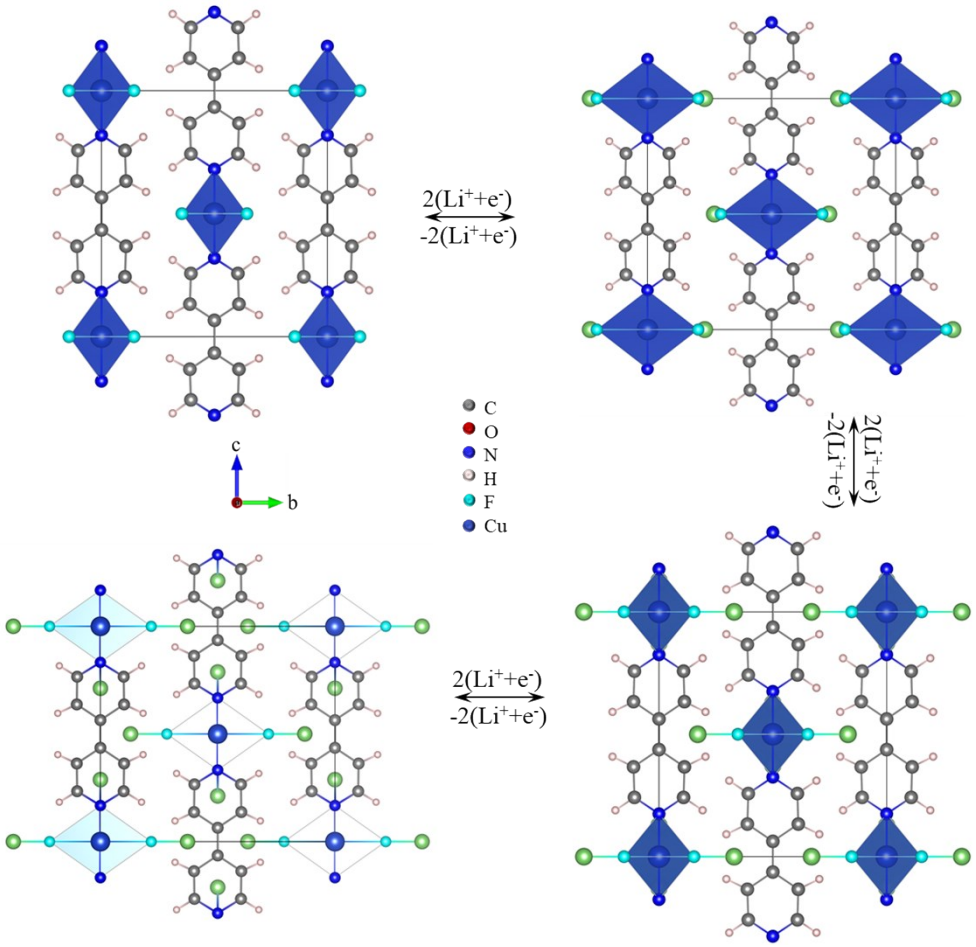

Figure S9. The Li-ions storage sites and the structural evolution in CuF_2(4,4′-bpy)

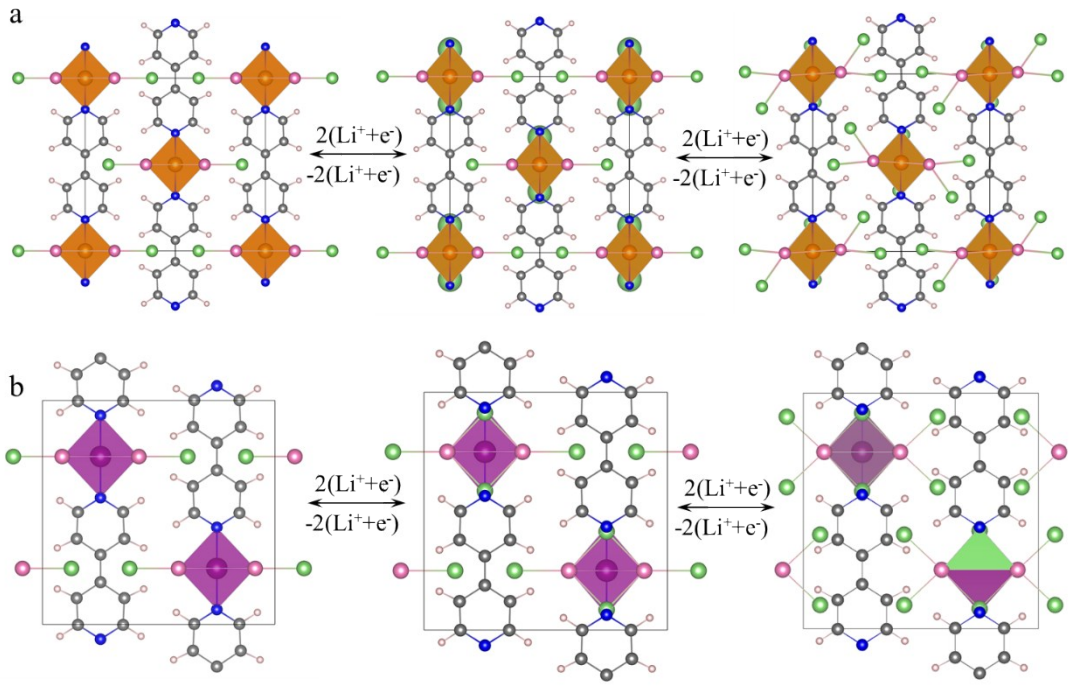

Figure S10. The Li-ions storage sites and the structural evolution in (a) $FeCl_2$(4,4′-bpy) and (b) $MnCl_2$(4,4′-bpy).

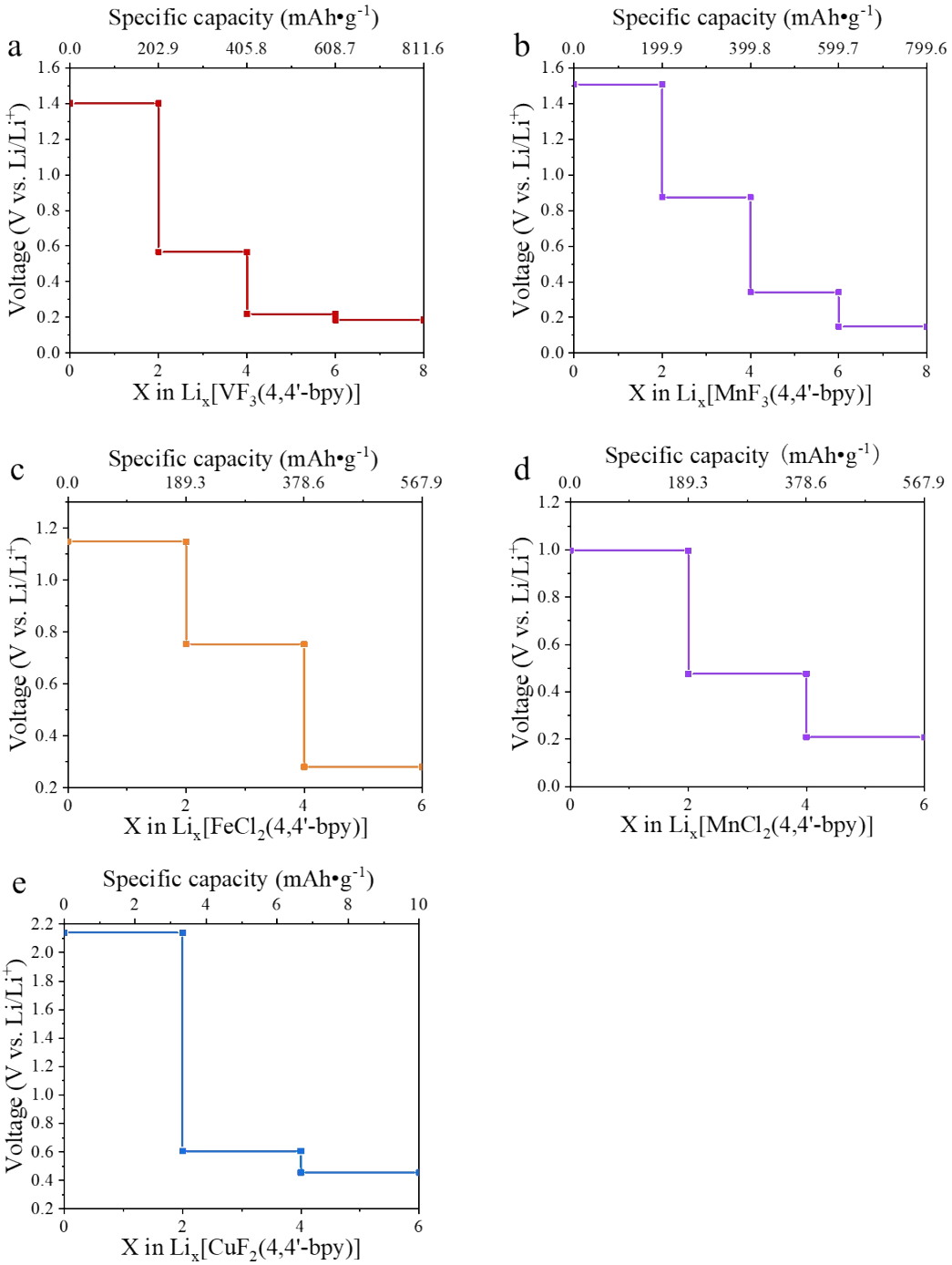

Figure S11. The voltages of (a) VF_3(4,4′-bpy), (b) MnF_3(4,4′-bpy), (c) $FeCl_2$(4,4′-bpy), (d) $MnCl_2$(4,4′-bpy) and (e) CuF_2(4,4′-bpy) during the discharge.

Table S3. Comparison of the lattice parameters of TMF_3(4,4′-bpy) (TM=Fe, V, Mn) and $TMCl_2$(4,4′-bpy) (TM=Fe, Mn) and the bond lengths of TM-F/Cl/N that were calculated by DFT and DFT+*U*.

Materials	Method	Lattice parameters				Bond length/Å	
		a/Å	b/Å	c/Å	α=β=γ/°	TM-F/Cl	TM-N
FeF_3(4,4′-bpy)	DFT+*U* (U_{eff} = 3.9)	3.924	10.540	11.402	90	1.892	2.170
	DFT	3.927	10.545	11.406	90	1.891	2.172
	Experiment[1]	3.890	10.799	11.395	90	1.859	2.160
$FeCl_2$(4,4′-bpy)	DFT+*U* (U_{eff} = 3.9)	11.983	11.114	3.425	90	2.318	1.975
	DFT	11.976	11.114	3.422	90	2.318	1.975
	Experiment[2]	11.929	11.447	3.638	90	2.504	2.184
VF_3(4,4′-bpy)	DFT+*U* (U_{eff} = 3.3)	3.859	10.656	11.313	90	1.877	2.115
	DFT	3.858	10.648	11.315	90	1.877	2.116
	Experiment[3]	3.797	10.769	11.312	90	1.841	2.128
MnF_3(4,4′-bpy)	DFT+*U* (U_{eff} = 4.6)	10.483	11.415	3.941	90	1.834	2.175
	DFT	10.474	11.412	3.943	90	1.835	2.174
	Experiment[4]	10.703	11.383	3.941	90	1.793	2.160
$MnCl_2$(4,4′-bpy)	DFT+*U* (U_{eff} = 4.6)	11.581	11.878	3.612	90	2.536	2.237
	DFT	11.202	11.884	3.377	90	2.331	2.018
	Experiment[5]	11.641	11.955	3.678	90	2.552	2.276